7 Superconductivity and Magnetism

M. Angst (till November 2003), M. Bruun (till November 2003), D. Di Castro,
D.G. Eshchenko, H. Keller, R. Khasanov, S. Kohout, M. Mali (till November 2003),
J. Roos, A. Shengelaya, S. Strässle (since Mai 2003),
M. Eremin (visiting scientist), V.A. Ivanshin (visiting scientist), B. Kochelaev (visiting scientist),
T. Schneider (Titularprofessor), and K.A. Müller (Honorarprofessor)

in collaboration with:
ETH Zürich (K. Conder, J. Karpinski), Paul Scherrer Institute (PSI) (E. Morenzoni), IBM Rüschlikon Research Laboratory (J.G. Bednorz), Université de Genève (Ø. Fischer), University of Birmingham (E.M. Forgan), University of St. Andrews (S.L. Lee), University of Rome (A. Bianconi), Kazan State University (A. Dooglav, M.V. Eremin, B.I. Kochelaev), University of Belgrade (I.M. Savić), Institute of Low Temperature and Structure Research, Polish Academy of Sciences, Wroclaw (P.W. Klamut), Institute of Physics, Polish Academy of Sciences, Warsaw (R. Puzniak, A. Wisniewski), University of Tokyo (K. Kishio, T. Sasagawa, H. Takagi), Northern Illinois University, DeKalb (B. Dabrowski).

Our last years research activities were again aimed at the fundamental physical properties of non-conventional superconductors such as cuprate high-temperature superconductors (HTS) and magnesium diboride (MgB_2).

A main focus was put on the role of the electron-phonon interaction in the basic physics of these systems by investigating the effects of isotope substitution and hydrostatic pressure on the relevant superconducting parameters. Furthermore, new aspects related to charge inhomogeneity as a possible intrinsic property of the novel superconductors were explored by studying finite-size effects and signatures of an electronic phase separation. Applying the combination of microscopic techniques [*muon-spin rotation (conventional μSR and low energy LEμSR), nuclear magnetic resonance (NMR), nuclear quadrupole resonance (NQR), electron paramagnetic resonance (EPR)*] and bulk-type measurements [*SQUID and torque magnetometry, resistivity*] proved to be of great advantage in our investigations, which are described in more detail in the following.

7.1 Studies of isotope effects in novel superconductors

7.1.1 Direct observation of the oxygen isotope effect on the magnetic field penetration depth in optimally doped $YBa_2Cu_3O_{7-\delta}$

A direct way to explore the role of the electron-phonon interaction in HTS is to investigate the isotope effect on the in-plane penetration depth λ_{ab} [1; 2; 3]. We used the advantages of the low-energy μSR (LEμSR) technique, developed recently at the Paul Scherrer Institute (PSI) [4], for the direct measurement of the oxygen isotope ($^{16}O/^{18}O$) effect (OIE) on λ_{ab} in optimally doped $YBa_2Cu_3O_{7-\delta}$ films [5]. The principle of λ determination by using LEμSR is shown schematically in Fig. 7.1. Low-energy muons of tuneable energy can be implanted at a different and controllable depth z beneath the surface of the superconductor in the Meissner state. Due to the random nature of the muon scattering process, the implantation depths are distributed over a nanometer scale, and the implantation depth profile $n(z)$ depends on the muon energy [Fig. 7.1(a)]. Knowing the value of the mean implantation depth $\overline{z}$ the magnitude of the local field $B(\overline{z})$ is obtained from the muon spin precession frequency.

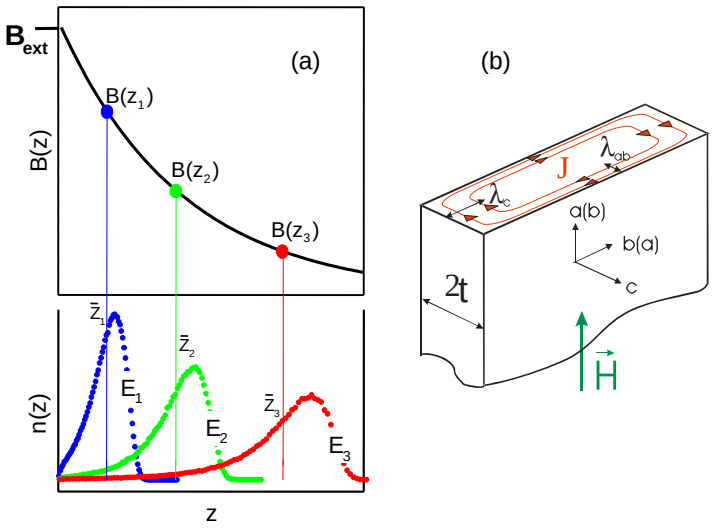

Figure 7.1:
(a) The principle of λ determination using LEμSR. By tuning the energy E of the incident muons they are implanted at controllable distances $\overline{z}$ beneath the surface of the superconductor in the Meissner state. The local magnetic field $B(\overline{z})$ is determined from the muon precession frequency using μSR. (b) Schematic distribution of the screening current J in a thin anisotropic superconducting slab of thickness $2t$ in a magnetic field applied parallel to the flat surface.

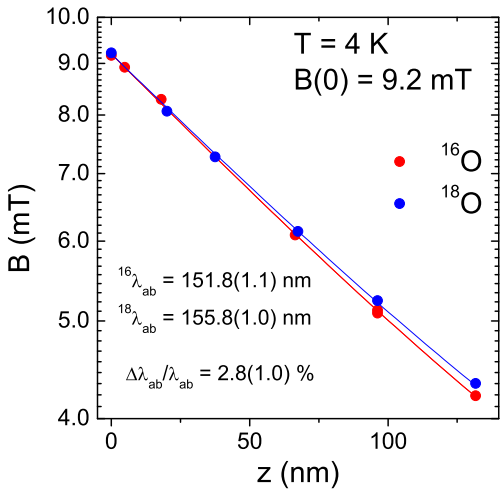

Figure 7.2: *Magnetic field penetration profiles $B(\overline{z})$ on a logarithmic scale for an ^{16}O substituted (red circles) and an ^{18}O substituted (blue circles) $YBa_2Cu_3O_{7-\delta}$ film measured in the Meissner state at 4 K and an external field of 9.2 mT, applied parallel to the surface of the film. The data are shown for implantation energies 3, 6, 10, 16, 22, and 29 keV starting from the surface of the sample. Solid curves are best fits by Eq. (7.1).*

The measurements of the in-plane magnetic penetration depth λ_{ab} were performed on a 600 nm thick epitaxial $YBa_2Cu_3O_{7-\delta}$ film in the Meissner state. A weak external magnetic field of 9.2 mT was applied parallel to the film surface after cooling in zero magnetic field from a temperature above T_c to 4 K. In this geometry (the thickness of the sample is negligible in comparison with the width), currents flowing in the ab-planes determine the magnetic field profile along the crystal c-axis inside the film [see Fig. 7.1(b)]. Spin-polarized muons were implanted at a depth ranging from 20-150 nm beneath the surface of the film by varying the energy of the incident muons from 3 to 30 keV. The muon implantation depth profile $n(z)$ for the given implantation energy was calculated using the Monte-Carlo code TRIM.SP [6]. The reliability of the calculated $n(z)$ was demonstrated by previous LEμSR experiments on thin metal layers [7].
For each implantation energy the average value of the magnetic field $\overline{B}$ and the corresponding average value of the stopping distance $\overline{z}$ were extracted. The value of $\overline{B}$ was taken from the fit of the μSR time spectrum assuming a Gaussian relaxation function. The value of $\overline{z}$ was taken as the first moment of the emulated $n(z)$ distribution. Results of this analysis for the ^{16}O and ^{18}O substituted $YBa_2Cu_3O_{7-\delta}$ films are shown in Fig. 7.2. The data points for the ^{18}O film are systematically lower than those for the ^{16}O film, showing that $^{16}\lambda_{ab} < {}^{18}\lambda_{ab}$. The solid lines represent a fit to the $B(\overline{z})$ data by the function:

$$B(z) = B_0 \frac{\cosh[(t-z)/\lambda_{ab}]}{\cosh(t/\lambda_{ab})}\,, \tag{7.1}$$

where $B(0)$ is the field at the surface of the superconductor, and $2t$ is the film thickness. Fits of Eq. (7.1) to the extracted $^{16}B(\overline{z})$ and $^{18}B(\overline{z})$ yield $^{16}\lambda_{ab}(4K) = 151.8(1.1)$ nm and $^{18}\lambda_{ab}(4K) = 155.8(1.0)$ nm. Taking into account an ^{18}O content of 95%, the relative shift was found to be $\Delta\lambda_{ab}/\lambda_{ab} = 2.8(1.0)\%$ at 4 K.

To confirm that the observed OIE on λ_{ab} is intrinsic, additional measurements of the Meissner fraction in fine powder samples with an average grain size compatible to λ_{ab} were performed. Analyzing the data using the procedure described in Ref. [1] gives $\Delta\lambda_{ab}/\lambda_{ab} = 2.7(1.0)\%$, in agreement with the LEμSR results. It was pointed out [1; 2; 3; 5] that the OIE on λ_{ab} arises mainly from the oxygen-mass dependence of the in-plane effective mass m^*_{ab}. Therefore, our finding implies that even in optimally doped HTS for which only a small isotope effect on T_c is observed, the supercarriers are strongly coupled to the lattice.

[1] G.M. Zhao *et al.*, Nature (London) **385**, 236 (1997).

[2] J. Hofer *et al.*, Phys. Rev. Lett. **84**, 4192 (2000).

[3] R. Khasanov *et al.*, J. Phys.: Condens Matter **15**, L17 (2003).

[4] E. Morenzoni *et al.*, J. Appl. Phys. **81**, 3340 (1997).

[5] R. Khasanov *et al.*, Phys. Rev. Lett. **92**, 057602 (2004).

[6] W. Eckstein, Computer Simulations of Ion-Solid Interactions (Springer-Verlag, Berlin, 1992).

[7] E. Morenzoni *et al.*, Nucl. Instrum. Methods B, **192**, 254 (2002).

7.1.2 Site-selective oxygen isotope effect on the penetration depth in $Y_{0.6}Pr_{0.4}Ba_2Cu_3O_{7-\delta}$

The observation of an OIE on λ_{ab} in HTS indicates an unusual (e.g., non-adiabatic) coupling of the electrons to phonon modes involving the movement of the isotope substituted atoms. It is important to identify the relevant phonon modes responsible for this effect. This can be achieved by investigating the site-selective oxygen-isotope effect (SOIE). We used transverse-field μSR to study the SOIE on T_c and λ_{ab} in underdoped $Y_{0.6}Pr_{0.4}Ba_2Cu_3O_{7-\delta}$ powder samples [1].

In order to prepare oxygen site-selective samples a two-step exchange process was applied [2]. The following site-selective samples were prepared: $^{16}O_{pac}$, $^{18}O_{pac}$, $^{16}O_p^{18}O_{ac}$, and $^{18}O_p^{16}O_{ac}$ where indexes p, a and c denote planar (within CuO_2 planes), apical and chain oxygen, respectively. The site-selectivity of the oxygen exchange was checked by Raman spectroscopy confirming that the site-selective oxygen substitution is almost complete in all the samples. The μSR measurements were performed at PSI using the

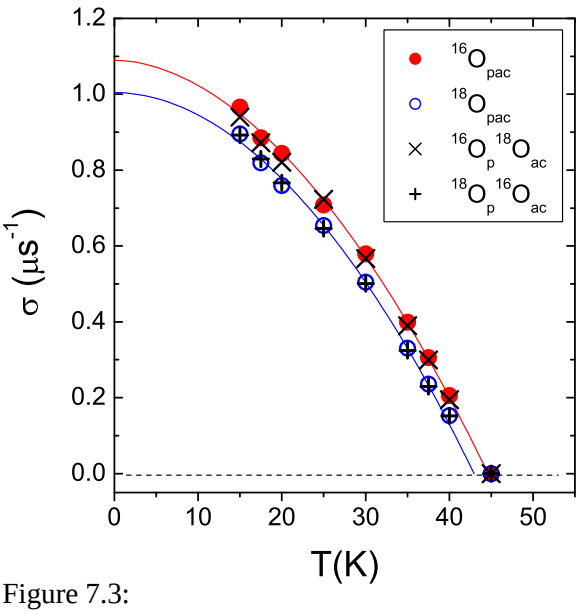

Figure 7.3:
Temperature dependence of the depolarization rate in site-selective $Y_{0.6}Pr_{0.4}Ba_2Cu_3O_{7-\delta}$ samples (200 mT, FC). The solid lines correspond to fits to the power law $\sigma(T)/\sigma(0) = 1 - (T/T_c)^n$ for the $^{16}O_{pac}$ and $^{18}O_{pac}$ samples.

πM3 beam line. The samples were cooled from far above T_c in a magnetic field of 200 mT. In a highly anisotropic layered superconductor the in-plane penetration depth λ_{ab} can be extracted from the muon-spin depolarization rate $\sigma(T) \propto 1/\lambda_{ab}^2$ which probes the second moment of the probability distribution of the local magnetic field function $p(B)$ in the mixed state [3]. The depolarization rate σ was extracted from the μSR time spectra using a Gaussian relaxation function. Figure 7.3 shows the temperature dependence of σ for the four $Y_{0.6}Pr_{0.4}Ba_2Cu_3O_{7-\delta}$ site-selective samples. It is evident that a remarkable oxygen isotope shift of T_c as well as of λ_{ab} is present. More importantly, the data points of the site-selective $^{16}O_p^{18}O_{ac}$ ($^{18}O_p^{16}O_{ac}$) samples coincide with those of the $^{16}O_{pac}$ ($^{18}O_{pac}$) samples. Therefore, our results show unambiguously that the OIE on both the transition temperature T_c and the in-plane magnetic penetration depth λ_{ab} comes from the oxygen within the superconducting CuO_2 planes and not from the apical and chain oxygen. Noting that the lattice parameters remain essentially unaffected by the isotope substitution [4], our results show the existence of a strong coupling of the electronic subsystem to phonon modes involving movements of the oxygen atoms in the CuO_2 plane, while suggesting that modes involving apical and chain oxygen are less strongly coupled to the electrons.

[1] R. Khasanov *et al.*, Phys. Rev. B **68**, 220506 (2003).

[2] K. Conder, Mater. Sci. Eng. **R32**, 41 (2001).

[3] P. Zimmermann *et al.*, Phys. Rev. B **52**, 541 (1995).

[4] F. Raffa *et al.*, Phys. Rev. Lett. **81**, 5912 (1998).

7.1.3 Finite-size and oxygen isotope effect in $Y_{0.6}Pr_{0.4}Ba_2Cu_3O_{7-\delta}$

Only in the ideal case superconductors can be considered as homogenous. For HTS there is increasing evidence that inhomogeneity is even an intrinsic property. Suppose that HTS are granular, consisting of spatial superconducting domains, embedded in a non-superconducting matrix and with spatial extent L_a, L_b and L_c along the crystallographic a, b and c-axes. The correlation length ξ_i in direction i, which increases strongly when T_c is approached, cannot grow beyond L_i. Consequently, for finite superconducting domains, thermodynamic quantities like the specific heat and penetration depth are smooth functions of temperature. As a remnant of the singularity at T_c these quantities exhibit a so-called finite size effect [1], namely a maximum or an inflection point at $T_{p_i(i=a,b,c)}$ (see Fig. 7.4). Knowing the value of T_{p_c} (see Fig. 7.4) and the values of the in-plane magnetic penetration depth λ_{ab} at $T = T_{p_c}$ the value of the domain size along c-direction L_c can be easily calculated[2]:

$$L_c = \frac{16\pi^3 k_B T_{p_c}}{\Phi_0^2} \frac{1}{\lambda_{ab}^{-2}(T_{p_c})} , \qquad (7.2)$$

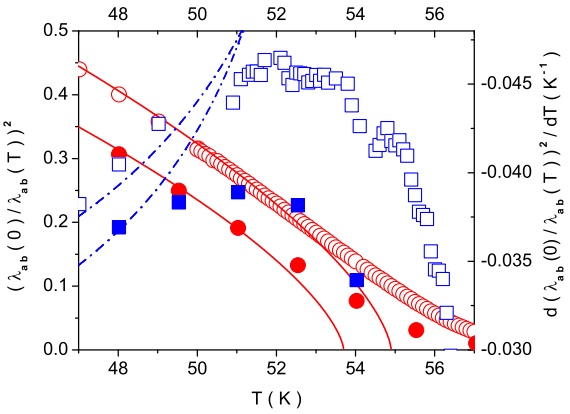

Figure 7.4: *Temperature dependence of the normalized $\lambda_{ab}^{-2}(T)/^{16}\lambda_{ab}^{-2}(0)$ in the vicinity of T_c for the ^{16}O – open circles and ^{18}O – closed circles $Y_{0.7}Pr_{0.3}Ba_2Cu_3O_{7-\delta}$ samples. Closed and open squares represent the temperature behavior of the first derivative $d\left(\lambda_{ab}^{-2}(T)/^{16}\lambda_{ab}^{-2}(0)\right)/dT$ for ^{16}O and ^{18}O substituted samples, respectively. The extrema in the first derivative around $T \approx 52.1(2)$ K and $51.0(2)$ K for ^{16}O and ^{18}O, respectively, clearly reveal the existence of an inflection point, characterizing the occurrence of a finite size effect in $1/\lambda_{ab}^2$. The solid and dashed lines indicate the leading critical behavior of a homogenous system with $L_c \sim \infty$.*

where Φ_0 is the flux quantum. The results of the finite size effect analysis in $^{16}O/^{18}O$ substituted $Y_{1-x}Pr_xBa_2Cu_3O_{7-\delta}$ ($x = 0.0$, 0.2, 0.3) samples are presented in Fig. 7.5, where the size of super conducting domains along the $c-$axis, L_c, versus the "inflection" temperature, T_{p_c}, are plotted. Two important points should be mentioned. (i) The domain size increases with decreasing T_{p_c} (T_c). This can be taken as an evidence for the shrinkage of limiting length scales upon change of doping, stemming from the behavior close to the quantum superconductor to insulator transition where T_c vanishes [3]. Here the cuprates become essentially two dimensional and correspond to a stack of independent slabs [4]. (ii) For a fixed Pr concentration the lattice parameters remain essentially unaffected by isotope substitution [5]. Accordingly, an electronic pairing mechanism, not taking into account coupling to local lattice distortions and anharmonic phonons, would imply $\Delta L_c = 0$. On the contrary, a significant change of L_c upon oxygen exchange uncovers the coupling to local lattice distortions and anharmonic phonons, involving the oxygen lattice degrees of freedom.

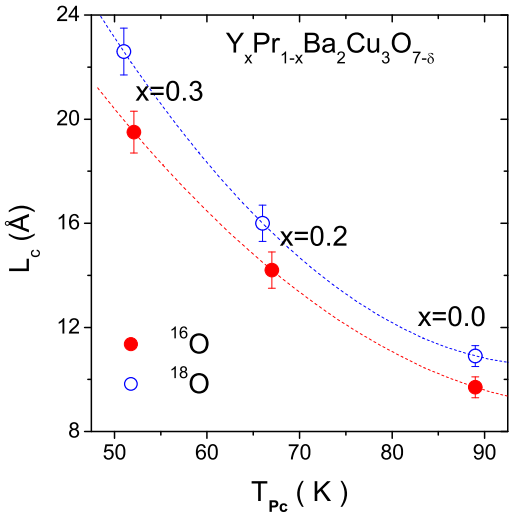

Figure 7.5: *Domain size L_c versus "inflection" temperature T_{p_c} for oxygen isotope $^{16}O/^{18}O$ substituted $Y_{1-x}Pr_xBa_2Cu_3O_{7-\delta}$ (x =0.0, 0.2, 0.3) samples. The dashed lines are guides to the eye.*

[1] M. E. Fisher and M. N. Barber, Phys. Rev. Lett. **28**, 1516 (1972).
[2] T. Schneider *et al.*, J. Phys.: Condens. Matter **15**, L763 (2003).
[3] T. Schneider, cond-mat/0210697.
[4] T. Schneider, Europhys. Lett. **60**, 141 (2002).
[5] F. Raffa *et al.*, Phys. Rev. Lett. **81**, 5912 (1998).

7.1.4 Isotope effect studies in magnesium diboride

The anomalous superconducting properties of MgB_2 such as, for example, specific heat and unusual behavior of the superconducting anisotropies, were explained by the existence of two sets of bands (π and σ) with different dimensionality and pairing strength. It was proposed [1; 2] that MgB_2 is a non-adiabatic superconductor, because of the strong coupling of the electrons to the E_{2g} phonon mode and the small Fermi energy. This would lead to the break-down of the *Migdal* adiabatic approximation, in which the density of states at the Fermi level, the electron-phonon coupling constant, and the effective supercarrier mass m^* are all independent of the mass M of the lattice atoms. To clarify this point, we continued a study of the boron isotope effect (BIE) on the magnetic penetration depth λ, a physical quantity directly related to the carriers effective mass m^*: $1/\lambda^2 \approx [\mu_0 e^2/c^2](n_s/m^*)$. Last year we obtained a BIE compatible with zero within the experimental error. To check the reproducibility of this result and to show that they are intrinsic for MgB_2, we repeated the experiment on samples of higher quality. To measure λ, we used again the μSR technique. For $Mg^{11}B_2$ and $Mg^{10}B_2$ isotope samples, we measured the temperature dependence of the muon spin depolarization rate σ, which is proportional to the second moment of the magnetic field distribution, and, under certain conditions, to the superfluid density $\sigma \propto 1/\lambda^2 \propto n_s/m^*$.

Therefore, a shift in $1/\lambda^2$ due to the isotope substitution would lead to a shift in m^*, since n_s does not change on isotope substitution.
In Fig. 7.6 the temperature dependence of σ for the new $Mg^{11}B_2$ and $Mg^{10}B_2$ isotope samples is reported. The data were fitted with the two-gap equation [3]:

$$\sigma(T) = \sigma(0) - w \cdot \delta\sigma(\Delta_1, T) - (1-w) \cdot \delta\sigma(\Delta_2, T), \tag{7.3}$$

with $\delta\sigma(\Delta,T)=\frac{2\sigma(0)}{k_B T}\int_0^\infty f(\varepsilon,T)\cdot[1-f(\varepsilon,T)]d\varepsilon$. Δ_1 and Δ_2 are the zero temperature large and small gaps, respectively, w is the relative contribution of the large gap to $\sigma(0)$, and $f(\varepsilon,T)$ is the Fermi distribution. For the temperature dependence $\Delta(T)$ of the gaps we used the conventional *BCS* gap function.

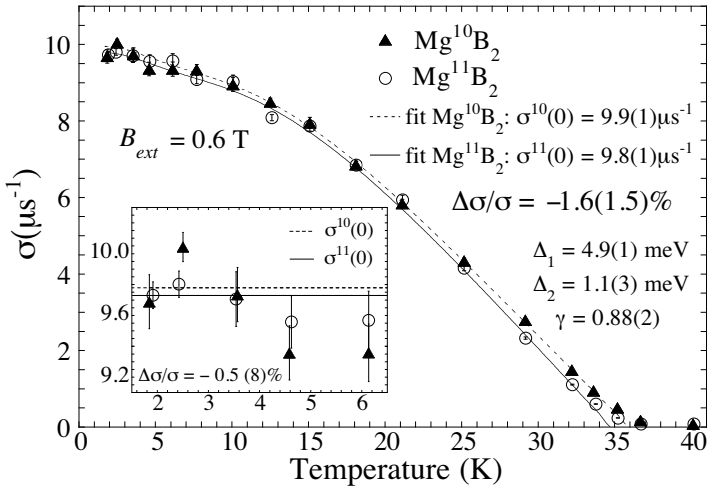

Figure 7.6: *Temperature dependence of the muon spin depolarization rate σ at $B_{\rm ext} = 0.6\,{\rm T}$ for the two isotope samples $Mg^{10}B_2$ (▲) and $Mg^{11}B_2$ (○). The solid ($Mg^{10}B_2$) and dotted ($Mg^{11}B_2$) lines are fits using Eq. (7.3). The inset shows the low-temperature region on a larger scale. The solid and dotted horizontal lines represent the weighted average values of $\sigma(0)$ for $T < 7.5\,{\rm K}$ for $Mg^{10}B_2$ and $Mg^{11}B_2$, respectively.*

From the fit we found $\Delta\lambda^2(0)/\lambda^2(0) = -1.6(1.5)\%$[3]. This result is in agreement with the previous one on samples of lower quality, showing that there is a negligible BIE on $\lambda^2(0)$. This is in contrast to the substantial oxygen isotope effect observed in the non-adiabatic cuprate HTS [4; 5]. Our results imply that polaronic or non-adiabatic effects in MgB_2 are absent or negligibly small. With this work we establish an upper limit to any theoretical prediction of such effects[1; 2].

[1] A. S. Alexandrov, Physica C **363**, 231 (2001).
[2] E. Cappelluti *et al.*, Phys. Rev. Lett. **88**, 117003 (2002).
[3] D. Di Castro *et al.*, cond-mat/0307330.
[4] J. Hofer *et al.*, Phys. Rev. Lett. **84**, 4192 (2000).
[5] R. Khasanov *et al.*, J. Phys.: Condens. Matter **15**, L17 (2003).

7.2 Studies of pressure effects in novel superconductors

7.2.1 Pressure effect on the penetration depth in $YBa_2Cu_4O_8$

Previous studies[1; 2; 3; 4] showed a substantial OIE on the in-plane penetration depth λ_{ab}, which indicates a non-adiabatic coupling of the electrons to phonon modes involving the movement of the isotope substituted atoms. Another way to study lattice effects are pressure experiments. The squeezing of the crystal lattice by external pressure changes the lattice parameters, the phonon spectrum and consequently the electron-lattice coupling. Surprisingly, the pressure effect on the magnetic field penetration depth has not attracted much attention so far.

Recently we performed the first measurements of the in-plane magnetic penetration depth λ_{ab} under high hydrostatic pressure (up to 11.5 kbar) in $YBa_2Cu_4O_8$. The temperature dependence of λ_{ab}^{-2} was extracted from Meissner fraction measurements at low magnetic field. A pronounced pressure effect on both the transition temperature T_c and $\lambda_{ab}^{-2}(0)$ is observed. Both quantities increase with increasing pressure. The pressure shift on $\lambda_{ab}^{-2}(0)$ can be attributed to (i) the pressure induced charge carrier transfer from chains to the planes and (ii) the decreasing of the in-plane charge carrier mass m_{ab}^*. However, it is demonstrated that the effect mainly ($\sim 2/3$) arises from the pressure dependence of m_{ab}^*.

[1] G.M. Zhao *et al.*, Nature (London) **385**, 236 (1997).

[2] J. Hofer *et al.*, Phys. Rev. Lett. **84**, 4192 (2000).

[3] R. Khasanov *et al.*, J. Phys.: Condens Matter **15**, L17 (2003).

[4] R. Khasanov *et al.*, Phys. Rev. Lett. **92**, 057602 (2004).

7.2.2 Pressure effect on the penetration depth in MgB_2

The pressure effect on the superconducting critical temperature T_c of MgB_2 has been studied at large. A linear pressure dependence was found, with dT_c/dP = 1.11(2) K/GPa [1]. It was attributed to the pressure induced lattice stiffening (increase of the phonon frequency) [2], rather than to the decrease in the electronic density of states. Comparison with theoretical calculations support the view that MgB_2 is a *BCS* superconductor with moderately strong electron-phonon coupling.
Apart from T_c, the most relevant superconducting parameter is the magnetic field penetration depth λ. A study of the pressure effect on $\lambda^{-2}(T=0)$, the so-called superfluid density, can give important information on how the electronic degrees of freedom are affected by lattice modifications and, therefore, on the nature of the electron-phonon coupling. In the cuprate HTS $YBa_2Cu_4O_8$, a large pressure effect on $\lambda^{-2}(0)$ was found (see section 7.2.2). Part of it can be attributed to the strong renormalization of the effective mass, due to the non-adiabatic coupling of the electrons to the lattice [3]. We studied the pressure effect on the magnetic penetration depth in the MgB_2 superconductor. The temperature dependence of $\lambda^{-2}(T)$ was extracted from the Meissner fraction measured in low magnetic field, and is plotted in Fig. 7.7 for two different pressures.

In analogy to our previous work [4], we fitted the experimental data at low temperature to a two-gap equation. The fit yields a very small pressure effect on $\lambda^{-2}(0)$: $\frac{\Delta\lambda^{-2}}{\lambda^{-2}} = -1.9(1.4)\%$. Our simple theoretical calculation of the pressure effect on λ [$\frac{\Delta\lambda^{-2}}{\lambda^{-2}} = -1.1\%$] confirms the experimental results, attributing the small pressure effect to a change in the stiffness of the Fermi velocity at low pressures. These results also confirm the adiabatic-like nature of the electron-phonon coupling, as it was revealed by the study of the boron isotope effect on $\lambda^{-2}(0)$ in MgB_2[4].

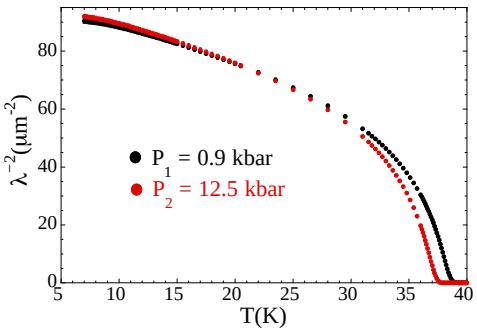

Figure 7.7: λ^{-2} *as a function of temperature for P = 0.09 GPa and 12.5 GPa.*

[1] T. Tomita *et al.*, Phys. Rev. B **64** (2001) 092505.

[2] F. Goncharov, Phys. Rev. B **64**, 100509(R) (2001).

[3] C. Grimaldi, E. Cappelluti, and L. Pietronero, Europhys. Lett. 42 , 667 (1998).

[4] D. Di Castro *et al.*, cond-mat/0307330.

7.3 Spectroscopic studies of novel superconductors

7.3.1 Low temperature NQR studies of $YBa_2Cu_4O_8$

In collaboration with the NMR group of the Kazan State University we continued our NQR study of the temperature dependent plane ^{63,65}Cu spin-lattice relaxation in superconducting $YBa_2Cu_4O_8$. In normal conducting $YBa_2Cu_4O_8$ the plane-copper spin-lattice relaxation is predominantly of magnetic origin caused by spin fluctuations and its temperature dependence is controlled by the spin-pseudogap phenomenon [1]. In the superconducting phase this magnetic contribution to the relaxation diminishes due to the opening of the superconducting gap. In previous measurements we have shown that with decreasing temperature this reduced relaxation changes its character and gets predominantly quadrupolar below 5 K with an unexpected temperature dependence [2]. The cause for this behavior is the appearance of new low frequency charge fluctuations at low temperatures. As a consequence of these new findings we extended the temperature range of our NQR spin-lattice relaxation measurements into the milli-Kelvin region. Fig. 7.8 shows the experimental results we obtained for ^{16}O and ^{18}O exchanged $YBa_2Cu_4O_8$.

Below 5 K the temperature dependence of the quadrupolar spin-lattice relaxation is characterized by a rate maximum at about 300 mK. This is a clear sign of a slowing-down of the dynamics of conjectured new charge inhomogeneities as e.g. stripe-like electronic structures. In a tentative model we can quantitatively describe the observed behavior by a distribution of charge fluctuation correlation times. Assuming thermally activated underlying processes it may be related to a distribution of energy barriers. A possible oxygen isotope effect on the details of the rate maximum is obscured by the errors of the data.

The slowing-down of dynamics is accompanied by a progressive reduction in the observed signal intensity of plane Cu nuclei (see Fig. 7.9). For the fully stoichiometric $YBa_2Cu_4O_8$ this phenomenon is observed for the first time. It seems similar to the so-called "wipe-out effect" observed in the LaSrCuO system (see e.g. [3]) but occurs at much lower temperatures. More detailed investigations are needed to clarify the origin of charge inhomogeneities in $YBa_2Cu_4O_8$ and have been started with a study of the temperature dependence of the plane Cu NQR relaxation behavior at very low temperatures in Ca doped $Y_{0.938}Ba_{1.962}Ca_{0.1}Cu_4O_8$.

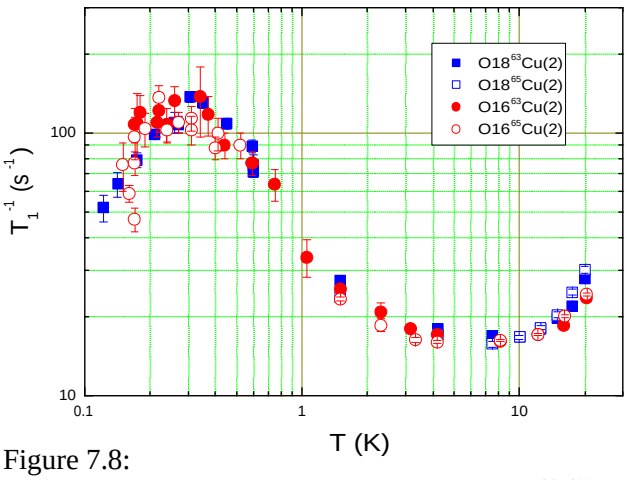

Figure 7.8:
Low temperature behaviour of the plane-^{63,65}Cu spin-lattice relaxation in ^{16}O and ^{18}O exchanged $YBa_2Cu_4O_8$.

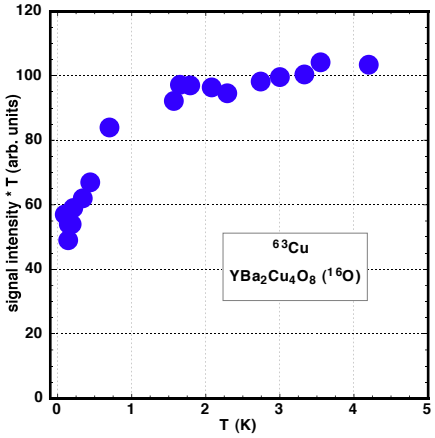

Figure 7.9:
Low temperature behaviour of the normalized plane ^{63}Cu NQR signal intensity of ^{16}O $YBa_2Cu_4O_8$.

[1] F. Raffa *et al.*, Phys. Rev. Lett. **81**, 5912 (1998).
[2] M. Mali *et al.*, Journal of Superconductivity: Incorporating Novel Magnetism **15**, 511 (2002).
[3] A. W. Hunt *et al.*, Phys. Rev. Lett. **82**, 4300 (1999).

7.3.2 NMR investigation of a MgB_2 single crystal

So far NMR investigations of MgB_2 have been performed exclusively by using polycrystalline samples. Regarding the superconducting phase in MgB_2 ($T_c = 39\,\mathrm{K}$), it is therefore very difficult to obtain reliable information on NMR parameters (particularly the relaxation rates) [1] due to the random orientation of crystallites with respect to the applied magnetic field and the strong critical field anisotropy [2]. Because high-quality single crystals of MgB_2 of sub-millimeter size became available recently [3] we started a single crystal MgB_2 investigation using quadrupole perturbed ^{11}B NMR. The measurements were performed from 250 K down to 9 K in a field of 9 T, applied along the boron planes, and revealed a transition temperature $T_c(9\,T) \approx 23\,\mathrm{K}$. An adapted micro-coil version of the resonant circuit was built in order to overcome the sensitivity limitations due to the unfavorably small size of the crystals. In normal conducting MgB_2 the electric field gradient (EFG) and the magnetic shift tensors at the boron site were determined. Whereas our experimental values for the EFG are in agreement with available literature data, we can now provide first reliable values for the magnetic shift components parallel and perpendicular to the boron layer, which are not available from powder sample investigations.

The ^{11}B spin-lattice relaxation rate (see Fig. 7.10) and the nuclear dipolar coupling were measured in the whole temperature range. In the normal conducting phase the relaxation rate is slightly anisotropic and it shows the well-known *Korringa* temperature behavior. In the superconducting phase it decreases exponentially with decreasing temperature due the opening of the larger of the two superconducting gaps. Within experimental errors no evidence for a coherence peak (*Hebel-Slichter*-peak) [4] in the relaxation rate was found. This is in contrast to published results obtained in powder sample investigations [5].

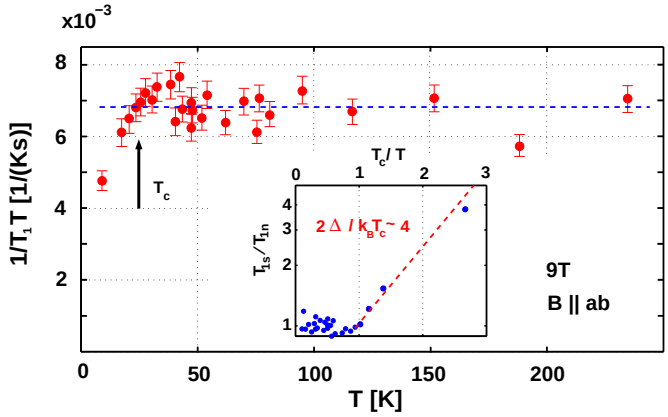

Figure 7.10: *Temperature dependence of the spin-lattice relaxation rate per unit temperature,* $1/T_1T$*. Insert: Plot of the ratio of* T_1 *in the superconducting phase and the normal phase against* T_c/T *showing the opening of the superconducting gap.*

[1] S.H. Baek *et al.*, Phys. Rev. B**66**, 104510 (2002).
[2] M. Angst *et al.*, Physica C**385**, 143 (2003).
[3] J. Karpinski *et al.*, Supercond. Sci. Technol. **16**, 221-230 (2003).
[4] L.C. Hebel and C.P. Slichter, Phys. Rev. **113**, 1504 (1959).
[5] H. Kotegawa *et al.*, Phys. Rev. Lett. **87**, 127001 (2001).

7.3.3 EPR study of lightly doped LaSrCuO

It is known that high-temperature superconductivity is achieved when a moderate density of conducting holes is introduced in the CuO_2 planes. At a critical concentration of doping $x_{cr} \approx 0.06$, superconductivity appears. However, it is still an unresolved issue how the electronic structure evolves with hole doping from the antiferromagnetic (AF) insulator to the paramagnetic metallic and superconducting state. While most of the theoretical models assume that the holes are homogeneously doped into CuO_2 planes, there is an increasing number of experiments pointing towards a highly nonuniform hole distribution leading to a formation of hole-rich and hole-poor regions [1]. This electronic phase separation is expected to be mostly pronounced at low hole concentrations. The Coulomb interaction limits the spatial extension of the electronic phase separation to hole-rich and hole-poor regions to a microscopic scale [2]. Therefore it is important to use a local microscopic method to study the electronic phase separation in cuprates. EPR is one of such methods.

We performed a thorough EPR investigation of the $La_{2-x}Sr_xCuO_4$ (LSCO) cuprate in the lightly doped range $0.01 \leq x \leq 0.06$, i.e. below x_{cr}. In order to observe the EPR signal, LSCO was doped with 2% of Mn^{2+} ions which replace the Cu ions in the copper-oxygen layer and serve as an EPR probe. The first important observation is that the EPR spectra consist of two lines. We found that they can be well fitted by a sum of two Lorentzian components with different linewidths: a narrow and a broad one.

Figure 7.11 shows the temperature dependence of the EPR intensity for the x=0.03 sample. One can see that the two EPR lines follow a completely different temperature dependence. The qualitatively different behavior of the broad and narrow EPR signals indicates that they belong to distinct regions in the sample. First we notice that the broad line vanishes at low temperatures. This can be explained by taking into account the AF order present in samples with very low Sr concentration [3]. In contrast to the broad line, the narrow signal appears at low temperatures and its intensity increases with decreasing temperature. This indicates that the narrow signal is due to the regions where the AF order is supressed. It is known that the AF order is destroyed by the doped holes, and above x = 0.06 AF fluctuations are much less pronounced [4]. Therefore, it is natural to relate the narrow line to regions with locally high carrier concentration and high mobility. Since we relate the narrow line to hole-rich regions, an exponential increase of its intensity at low temperatures indicates an energy gap for the existence of these regions.

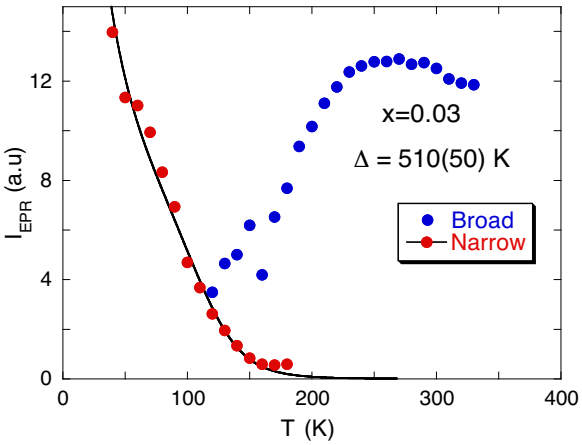

Figure 7.11: *Temperature dependence of the narrow and broad EPR signal intensity in* $La_{2-x}Sr_xCu_{0.98}Mn_{0.02}O_4$ *with* x = *0.03. The solid line represents a fit using the model described in the text.*

We propose a model where this microscopic phase separation is driven by the elastic interactions between the holes. This interaction is highly anisotropic being attractive for some orientations and repulsive for others [5]. The attraction between holes may result in a pair formation when holes approach each other closely enough. The pair formation can be a starting point for the creation of hole-rich regions by attracting additional holes. Because of the highly anisotropic elastic forces these regions are expected to have the form of stripes. Therefore the pair formation energy Δ can

be considered as an energy gap for the formation of hole-rich regions. The solid line in Fig. 7.11 represents a fit using this model. For the pair formation energy we obtained Δ = 460(50) K, which is practically doping-independent. This value agrees very well with the value of Δ obtained from the analysis of inelastic neutron-scattering and Raman data in cuprate HTS [6].

To summarize, performed EPR experiments provide a very important information about the electronic structure of the lightly-doped LSCO. First, we obtained a clear indication of the electronic phase separation into microscopic hole-rich and hole-poor regions. This shows that metallic domains exist in LSCO starting from very small carrier concentrations. A second important observation is the gap related with the formation of the metallic regions. The gap value extracted from our experiments is nearly the same as that deduced from other experiments for the formation of bipolarons [6], pointing to the origin of the metallic regions.

[1] See, for instance, *Phase separation in Cuprate Superconductors*, edited by K.A. Müller and G. Benedek (World Scientific, Singapore, 1993).
[2] V. J. Emery and S. A. Kivelson, Physica C **209**, 597 (1993).
[3] J. H. Cho *et al.*, Phys. Rev. Lett. **70**, 222 (1993).
[4] Ch. Niedermayer *et al.*, Phys. Rev. Lett. **80**, 3843 (1998).
[5] B. I. Kochelaev *et al.*, Mod. Phys. Lett. B**17**, 415 (2003).
[6] V. V. Kabanov and D. Mihailovic, Phys. Rev. B**65**, 212508 (2002).

7.3.4 Tri-layer Y123/Pr123/Y123 studies by means of LEμSR

There are several motivations behind the study of high-T_c multilayered structures. First, there is a technological need for heterostructures containing superconductors and insulating (or metallic) layers, for instance in the fabrication of Josephson and proximity effect junctions. Second, multilayers have been demonstrated in the past to be very powerful tools for studying the basic physics of semiconductors [1] and metals [2].

The low-energy-muon technique available at PSI is well suited for such a multilayer study: slow muons of tunable energy between 1 keV and 30 keV can be implanted at a very small and controllable depth below the surface of a sample. This allows all the advantages of standard μSR to be obtained in thin samples, near surfaces, and as a function of depth below surfaces [3]. We started the project with the simplest system of a 33 nm/50 nm/ 115 nm $YBa_2Cu_3O_7$/$PrBa_2Cu_3O_7$/$YBa_2Cu_3O_7$ (Y123/ Pr123/ Y123) structure grown at the Université de Genève. Our first μSR measurements in zero magnetic field are presented in Fig. 7.12.

Implantation energies of incoming muons were tuned to stop most of the muons in the appropriate layer (3 keV/12.5 keV/30 keV). In the top Y123 layer, we observed a slowly relaxing signal (due to the copper nuclear moments). The precession signal seen in the intermediate layer indicates that Pr123 is in an antiferromagnetic state with an internal field $B_{int} \sim 150$ G. We see no significant change in the internal field measured at T=110 K (which is above the superconducting transition for bulk Y123) and at T=5 K, respectively. The value observed is similar to the internal magnetic field known for bulk Pr123 at $T \sim 100$ K. At 30 keV most of the muons stop inside the last Y123 layer and give rise to the slow relaxing signal. The small additional precession signal seen in this spectrum corresponds to a small part of the muons which are still stopped in the antiferromagnetic intermediate layer. Zero field measurements confirmed the good quality of the tri-layer film and demonstrate the capability of the low-energy-muon technique. We also started measurements in a weak ($H < H_{c1}$) external

field applied parallel to the surface of the film. A preliminary analysis shows that the magnetic field measured inside both of the Y123 layers is screened better than it is estimated for separated Y123 layers in the Meissner state. This finding requires further experimental study. In particular we are planing experiments in single thin films of Pr123 and Y123.

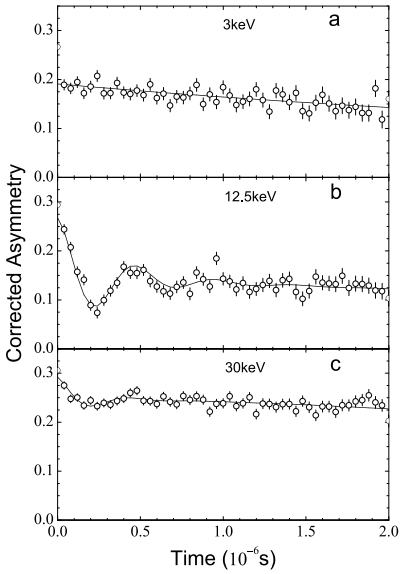

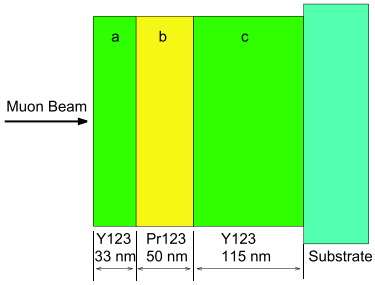

Figure 7.12: *Experimental μSR spectra measured at $T = 25\,K$ in zero magnetic field in:*
a) first $YBa_2Cu_3O_7$ layer;
b) intermediate $PrBa_2Cu_3O_7$ layer;
c) second $YBa_2Cu_3O_7$ layer.

[1] L. Esaki in *Synthetic Modulated Structures*, ed. by L.L. Chang and B.C. Giessen (Academic Press, New York, 1985), ch. 1.

[2] C.M. L. Falco and I.K. Schuller in *Synthetic Modulated Structures*, ed. by L.L. Chang and B.C. Giessen (Academic Press, New York, 1985), ch. 9,10.

[3] Morenzoni *et al.*, J. Appl. Phys. 81, 3340 (1997).

7.4 Magnetometry of cuprate superconductors

7.4.1 Doping dependence of superconducting properties of LaSrCuO by torque measurements

In continuation of our former projects we are working on the measurement of oxygen isotope effects in cuprate single crystals. As the isotope exchange occurs by diffusion of the oxygen within the sample, crystals used for this kind of study need to be very small (on the order of $150\,\mu m$ along each direction) to ensure a complete exchange. This rises the need for very sensitive equipment capable of measuring the small effects (below $5\,\%$) associated with isotope exchange experiments. In this case the torque magnetometer developed in our group specifically for this purpose is used. In a torque experiment a magnetic sample is exposed to an external magnetic field and the mechanical torque is measured as a function of temperature, and the applied field's magnitude and direction. Due to their anisotropy cuprate superconductors are well suited for this kind of study. Depending on the used theoretical models several superconducting properties such as the critical temperature T_c, the magnetic penetration depth λ, the correlation length ξ or the anisotropy parameter γ can be calculated from appropriate torque measurements.

Our interest lies in the investigation of the cuprate superconductor $La_{2-x}Sr_xCuO_4$ covering the whole doping regime from underdoped to overdoped samples with critical temperatures ranging from $18\,$K to $35\,$K. The field dependent measurements at a fixed field orientation (angle between the magnetic field and the samples main axis $\theta = 45°$) collected up to now can be used to extract some superconducting properties, but more measurements at different angles are needed to reliably determine all properties of interest. As an example the in-plane correlation length ξ_{ab} is shown in Fig. 7.13 as a function of temperature for the differently doped single crystals. The divergence close to T_c is well visible.

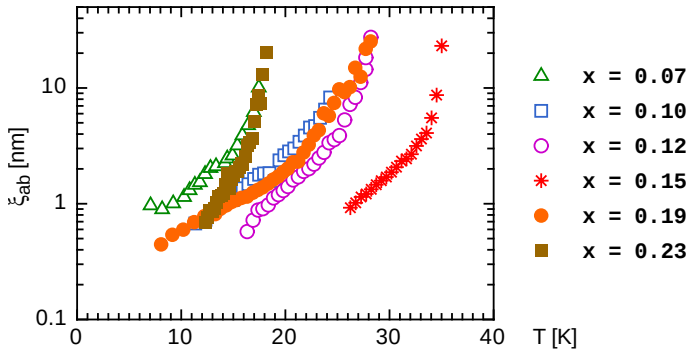

Figure 7.13:
Temperature dependence of the in-plane correlation length ξ_{ab} of $La_{2-x}Sr_xCuO_4$ for different doping levels x.

7.4.2 Anisotropy and internal field distribution of MgB_2 in the mixed state at low temperatures

The two-band superconductivity in MgB_2 leads to an array of unusual superconducting properties, particularly to a very unusual behavior of the superconducting anisotropies [1]. For example, a pronounced temperature dependence of the anisotropy γ_H of the upper critical field H_{c2}, directly related to the coherence length ξ, was observed [2] and calculated based on the two-band model [3]. In comparison, calculated values of the low field penetration depth anisotropy, γ_λ, are much lower, with an opposite temperature dependence [4]. This was experimentally confirmed as well by measurements of H_{c1} [5] and investigations by small-angle neutron scattering [6]. However, experiments indicate that, γ_λ is close to isotropicin the limit of very low fields, whereas it is soon rising strongly with increasing field H [6].

The behavior of the anisotropies of the superconducting length scales in the mixed state $H_{c1} < H < H_{c2}$ still needs to be clarified. Therefore, to study the field dependence of the anisotropy at low temperature, we analyzed SQUID and torque magnetization data, obtained from a MgB_2 single crystal with very low pinning, and μSR data, measured on unaligned MgB_2 powder. We determined the field dependence of the magnetic penetration depth, which is obtained from the field or angle dependence of the bulk magnetization (SQUID/torque), as well as from the average variation of the internal field (μSR).

The results from SQUID and μSR measurements are consistent in showing a rapid decrease of the superfluid density, $1/\lambda^2$, with the field H increasing below about 10 kOe (see Fig. 7.14). Moreover, both SQUID and torque data agree on the anisotropy γ_λ, increasing strongly with H as shown in Fig. 7.15. The analysis of the torque data further suggests that the coherence length anisotropy is not very different from the one of the penetration depth in any given field.

These findings are consistent with the decrease of the contribution to super-

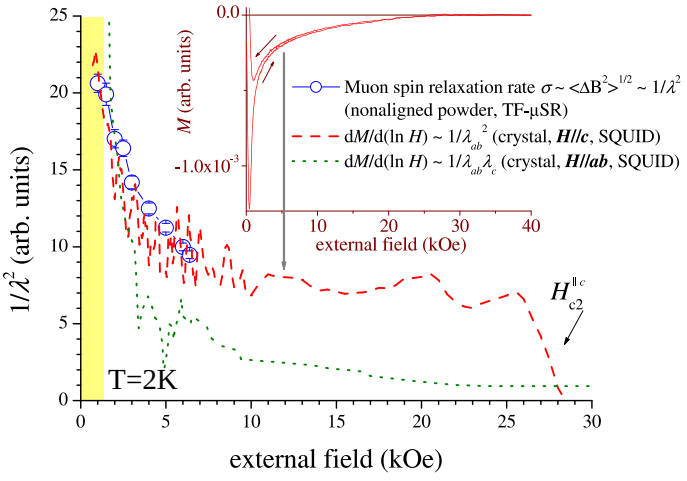

Figure 7.14: *Comparison of λ^{-2} vs H obtained from $dM/dlnH$ from SQUID measurements on a single crystal with $H//c$ (dashed curve) and $H//ab$ (dotted curve) and from the muon spin depolarization rate measured on unaligned powder (open circles). The shaded box indicates fields close to or lower than H_{c1}. Inset: $M(H)$ measured on the crystal with $H//c$.*

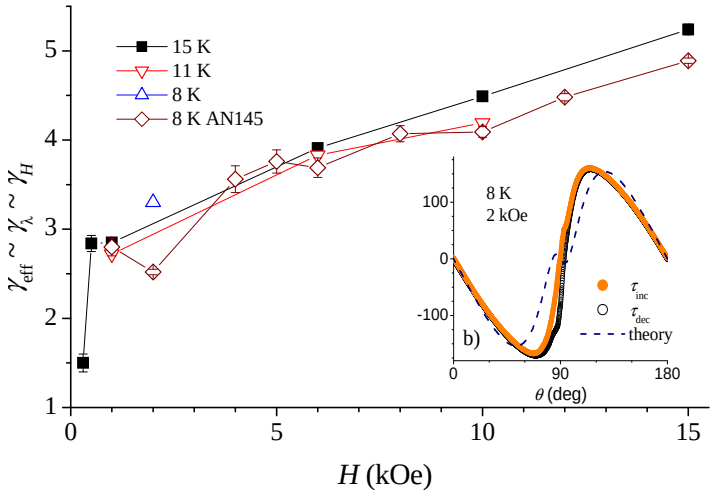

Figure 7.15: *Anisotropy as determined from an analysis of angle dependent torque data at various low temperatures, as a function of the applied field. Inset: Angle dependence of torque in 2 kOe at 8 K. The dashed line is a theoretical description, assuming* $\gamma_\lambda \ll \gamma_H$.

conductivity of the more isotropic π band, which has lower intrinsic H_{c2}^{π} in respect of the anisotropic σ band. The data presented indicate that H_{c2}^{π} is manifested by a rather broad crossover.

[1] M. Angst and R. Puzniak, in Focus on Superconductivity Research 2003, edited by B. P. Martines (Nova Publishers, New York, 2004), Chap. 1, preprint on cond-mat/0305048.

[2] M. Angst *et al.*, Phys. Rev. Lett. **88**, 167004 (2002).

[3] A. A. and A. E. Koshelev, Phys. Rev. B **68**,104503 (2003).

[4] V. G. Kogan, Phys. Rev. B **66**, 020509 (2002).

[5] L. Lyard *et al.*, Phys. Rev. Lett. **92**, 057001 (2004).

[6] R. Cubitt *et al.*, Phys. Rev. Lett. **91**, 047002 (2003).